IET Microwaves, Antennas & Propagation

Research Article

Mobile antenna performance improvement by ground mode tuning using a closed loop

ISSN 1751-8725
Received on 4th August 2016
Revised 12th January 2017
Accepted on 8th February 2017
E-First on 24th May 2017
doi: 10.1049/iet-map.2016.0638
www.ietdl.org

Sangmoon Yoo[1], Longyue Qu[1], Joonchul Kim[1], Hyeongdong Kim[1] ✉
[1]*Department of Electronic Engineering, Hanyang University, 222 Wangsimni-ro, Seongdong-gu, Seoul, Republic of Korea*
✉ *E-mail: hdkim@hanyang.ac.kr*

Abstract: An antenna with a modified ground plane is proposed for modern mobile devices in the wireless communications. The proposed antenna design comprises a planar inverted-F antenna with a feeding capacitor (C_F) at the top side of the ground plane, and an additional closed loop with lumped inductors (L_1 and L_2) at the end of the ground plane. The closed loop is connected to the small ground plane for ground mode tuning so that the ground mode resonant frequency is equal to the operating frequency. In the simulation, the −10 dB bandwidth is 140 MHz (from 2.39 to 2.53 GHz) without the closed loop, and is 320 MHz (from 2.34 to 2.66 GHz) with the proposed closed loop. The measured efficiency is 61% on average from 2.3 to 2.6 GHz for the proposed antenna, and is 36% for the reference antenna. The ground mode resonance can be easily tuned, and the proposed technique is a versatile approach for antenna performance improvement.

1 Introduction

Due to the rapid growth in the wireless communications market, antenna design has attracted significant interest. Features have been added to each new generation of wireless systems while mobile devices have become progressively smaller. This miniaturisation of wireless communication devices has created a high demand for, antenna characteristics of small size, wide impedance bandwidth and high efficiency, especially for mobile antennas. Many previous studies have focused on antenna miniaturisation [1–3]. However, the well-known Chu-Harrington limit [4–7] means the antenna performance of an ideally small antenna is approximately inversely proportional to the volume of the antenna in wavelength, and its impedance bandwidth is limited by the size of the antenna. Electrical small antennas suffer from high Q narrow impedance bandwidth, and low efficiency, so that good antenna performance is difficult to achieve. Therefore, a great challenge for antenna engineers is to develop a small antenna with good antenna performance. Furthermore, it is known that the ground plane has been proved to be a good radiator, and the antenna performance of a mobile antenna can be improved by enhancing the coupling between the antenna and the ground plane [8–10].

The ground mode resonance is tuned by simply adding a small closed loop at the end of the ground plane to improve the antenna performance of a conventional planar inverted-F antenna (PIFA). The closed loop is connected to the ground plane for open-end extension, and lumped inductors are adopted for easy control. We demonstrate that the optimal radiation performance can be achieved when the ground mode resonance frequency is equal to the antenna operating frequency. This paper is organised as follows. In Section 2, we describe the reference and proposed antenna configurations, and we explain the theoretical analysis using the equivalent circuit model of the antenna and ground plane. In Section 3, we present the controlling mechanism and the parametric studies for ground mode tuning. The antenna performance as verified by the experimental results is discussed in Section 4. We thus show that antenna performance can be significantly improved by using a small closed loop that has easy fabrication, tunability and applicability to various frequency bands. The proposed antenna was simulated and then measured using Agilent 8753ES Network Analyzer and a 6 m × 3 m × 3 m three-dimensional anechoic chamber.

2 Antenna design and theoretical analysis

The proposed technique is tested and verified with a PIFA for the 2.4 GHz wireless local area network (WLAN) band. The geometry of the reference and proposed antennas is shown in Fig. 1. A 30 mm × 20 mm ground plane is etched on the top layer of a flame retardant type 4 substrate ($\varepsilon_r = 4.4$, $\tan\delta = 0.02$, thickness = 1 mm). The PIFA is located at the top side of the ground plane in a compact size of 4 mm × 18 mm, and the antenna is fed by a feeding loop in series with a capacitor (C_F), so that the impedance matching can be conveniently controlled by the value of C_F without changing the feeding structure. The values of C_F for the reference design and proposed design are 0.3 and 0.4 pF, respectively. The proposed closed loop is located at the bottom of the ground plane with a compact size of W mm × 20 mm ($W = 4$ mm) where W is the width of the closed loop. The lumped inductors (L_1, L_2) are connected between the ground plane and the closed loop to enlarge the effective electrical size of the ground plane without changing the size of the loop. The lumped inductors are connected between the ground plane and the closed loop to enlarge the effective electrical size of the ground plane without changing the size of the loop. In the proposed design, the width of the conducting traces in the antenna and the closed loop is 1 mm. In this paper, the lumped inductors (L_1, L_2) and capacitor (C_F) are assumed to be lossless in simulation. In experiment, Murata 0402 LQG series chip inductors with Q-factor = 40 and Murata 0402 GRM series chip capacitors with Q-factor = 410 are used.

The PIFA operates as an electric dipole antenna and can have strong coupling with the ground plane when it is located near the electric field maximum of the ground plane (i.e. at the end of the ground plane), so the ground plane is efficiently excited as a dipole-type radiator [11, 12]. However, the length of the ground plane is much smaller than a half wavelength, indicating that the resonance frequency of the ground plane is significantly higher than the antenna operating frequency. Therefore, the ground plane mode cannot be strongly excited due to small coupling with the electric dipole antenna, so the impedance bandwidth is narrow and the radiation efficiency is low. To achieve stronger coupling, we added the proposed close loop at the end of the ground plane to tune the resonance frequency of the ground plane. Lumped inductors are connected with the closed loop to achieve compact size and easy tunability. Therefore, when the resonance frequency of the ground plane is tuned to the operating frequency, optimal coupling and optimal impedance bandwidth can be obtained [13–16].

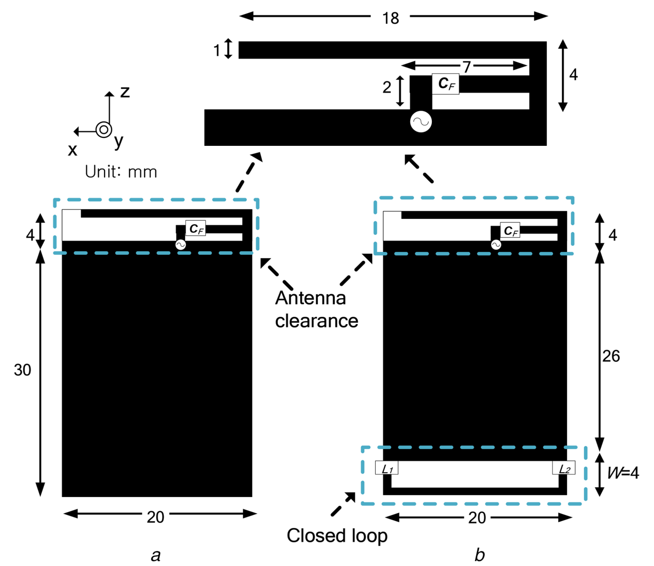

Fig. 1 *Geometry of the reference and proposed antennas*
(a) Reference antenna, ***(b)*** Proposed antenna

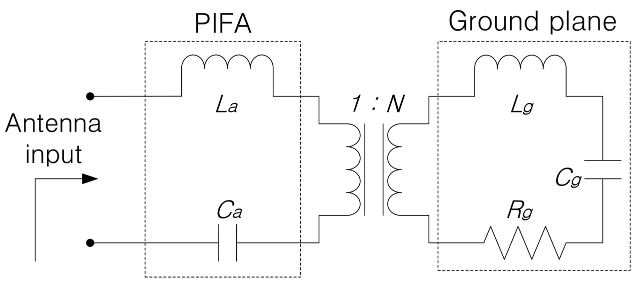

Fig. 2 *Equivalent circuit model between the antenna and the ground plane*

To understand the proposed technique, an equivalent circuit between the ground plane and the antenna is modelled as shown in Fig. 2. The PIFA is simply represented by a series circuit with inductance L_a and capacitance C_a, while the ground plane is modelled with L_g, C_g and resistance R_g. N is the coupling factor defined by the mutual coupling between the conventional PIFA and the ground plane [12]. The input power from the antenna is coupled to the ground plane so that radiation is generated. It is noted that different types of the antenna structure can be used for exciting the characteristic mode, such as the ground radiation antenna (GradiAnt) and loop-type antennas [17–19].

The input impedance of the equivalent circuit model without the closed loop can be mathematically expressed as [11, 14]

$$\begin{aligned} Z_{\text{in}} &= \text{j}\omega L_a + \frac{1}{\text{j}\omega C_a} + \frac{N^2}{\text{j}\omega L_g + (1/\text{j}\omega C_g) + R_g} \\ &= \text{j}Q_a\left(\frac{\omega}{\omega_a} - \frac{\omega_a}{\omega}\right) + \frac{N^2}{R_g\left[1 + \text{j}Q_g\left((\omega/\omega_g) - (\omega_g/\omega)\right)\right]} \end{aligned} \tag{1}$$

$$\omega_g = \frac{1}{\sqrt{L_g C_g}} \tag{2}$$

where Q_a is the unloaded quality factor of the antenna and Q_g is that of the ground plane. The first term of (1) is the impedance of the conventional PIFA, and the last term of (1) can be viewed as the mutual impedance due to the mutual coupling between the conventional PIFA and the ground plane. The ground mode resonance frequency can be defined by (2) so that the ground mode resonance can be tuned by the inductance L_g and capacitance C_g [20], which can explain the controlling mechanism of the inductor-connected closed loop. Meanwhile, the numerator N is the mutual coupling between the antenna and the ground plane as expressed above, which can be written as [12]

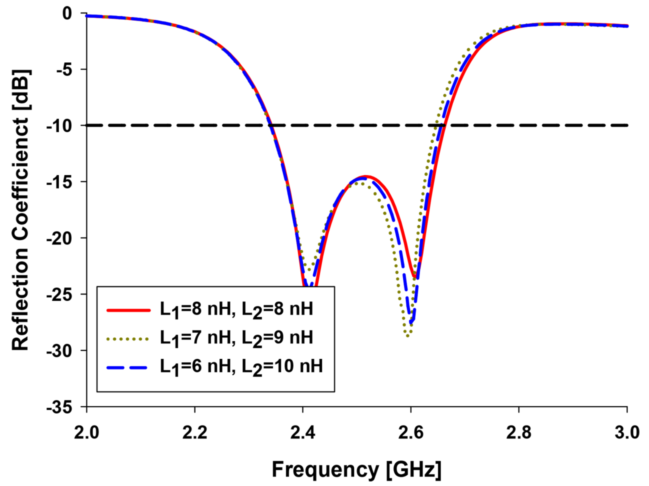

Fig. 3 *Simulated reflection coefficients with different values of L_1 and L_2*

$$N = \iiint \overline{E_0} \cdot \overline{J^i}\, \mathrm{d}\tau \tag{3}$$

where E_0 is the electric field distribution on the ground plane and J^i is the induced current distributions due to the antenna. ω_a and ω_g are the resonance frequencies of the antenna and the ground plane, respectively. Coupling is getting stronger as ω_g approaches ω_a. As more coupling is generated, more input power is coupled to the ground plane, thus both impedance bandwidth and radiation efficiency can be improved [13–16]. Equations (1)–(3) represent useful concepts for mobile antenna design, providing valuable insight for achieving optimal coupling between the antenna and the ground plane. Based on the above analysis, parasitic capacitance and inductance can be provided by the closed loop so that the resonance frequency of the ground plane is lowered. The best antenna performance is expected when the ground mode resonance is tuned to equal the operating frequency. The proposed closed loop can be a different shape and can be connected by lumped capacitors combined with lumped inductors. In addition, the proposed technique is versatile for different types of antennas and different operating frequencies.

3 Controlling mechanism and parametric studies

The lumped inductors (L_1, L_2) in the closed loop are important parameters for the ground mode tuning technique, and the values of L_1 and L_2 can be various combination. Based on the theoretical analysis above, it is known that the ground mode resonance is decided by the total value of L_1 and L_2, without considering the different combination. To further verify this, the simulated reflection coefficients are shown in Fig. 3 by setting L_1 and L_2 different values while keeping the sum values constant. It can be observed that the bandwidth and impedance matching barely changes when the sum value of L_1 and L_2 is constant. Therefore, it can be concluded that both L_1 and L_2 are altogether contributing to the change of the inductance L_g. For simplicity, the value of L_1 is set to be equal to that of L_2 (i.e. $L_1 = L_2 = 8$ nH).

Since the ground mode resonance does not change according the combination of L_1 and L_2, the antenna radiation efficiency does not vary with the combination. Therefore, the radiation efficiency variations at 2.45 GHz are studied in simulation as the values of $L_1 + L_2$ change while keeping $L_1 = L_2$, as shown in Fig. 4. It can be observed that the radiation efficiency varies as the value of $L_1 + L_2$ increases from 0 to 20 nH, and then decreases when $L_1 + L_2 = 20$ nH. When $L_1 + L_2 = 16$ nH, the maximum radiation efficiency of 91% is obtained. The simulated radiation efficiency of the reference antenna without the closed loop is 74%, indicating that great improvement is achieved by using the proposed closed loop.

The ground mode resonance controlling is demonstrated by the simulated input impedance in a Smith chart, as shown in Fig. 5*a*,

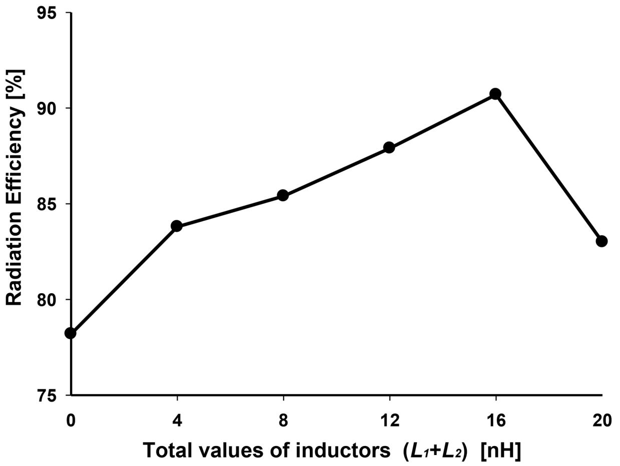

Fig. 4 *Simulated radiation efficiency variations with total inductors values ($L_1 + L_2$) at 2.45 GHz*

by changing the values of L_1 and L_2 from 7 to 9 nH. In these cases, the ground mode resonance ω_g is close to the operating frequency, so that strong coupling N is generated between the antenna and the ground plane, which can be observed by the ground mode resonance (small impedance locus in the Smith chart). It is interesting to see that the small locus rotates counter-clockwise as L_1 and L_2 increases, which can be explained by (2), where the ground mode resonance frequency can be controlled by the values of C_g or L_g. The closed loop increases the inductance and capacitance of the ground plane, especially the inductance due to the inductors L_1 and L_2. In Fig. 5*b*, the reflection coefficients in each case are shown accordingly. It can be observed that better impedance matching and dual resonance [21–23] has been obtained when the value of L_1 and L_2 is 8 nH.

The impedance matching controlling for the proposed technique is demonstrated by the simulated input impedance in a Smith chart, as shown in Fig. 6*a*, by changing the values of C_F from 0.3 to 0.5 pF. It can be obviously seen that the antenna resonance (the large impedance locus in the Smith chart marked by the arrows) gets larger as the value of C_F increases, and better impedance matching of the proposed antenna can be obtained when $C_F = 0.4$ pF. Fig. 6*b* shows the corresponding reflection coefficients when C_F changes, where the impedance bandwidth is 320 MHz when C_F is 0.4 pF, which is consistent with the input impedance in the Smith chart.

Fig. 7 shows simulated reflection coefficients for different widths (W) of the closed loop. The data are obtained without changing the value of C_F, but the impedance matching can be retuned when necessary. The values of W are varied from 2 to 4 mm, and it can be observed that the impedance bandwidth ranges from 250 MHz (2.36–2.61 GHz) to 280 MHz (2.34–2.61 GHz) as W varies from 2 to 3 mm. When W is enlarged to 4 mm, the impedance bandwidths is 320 MHz (2.34–2.66 GHz) providing the

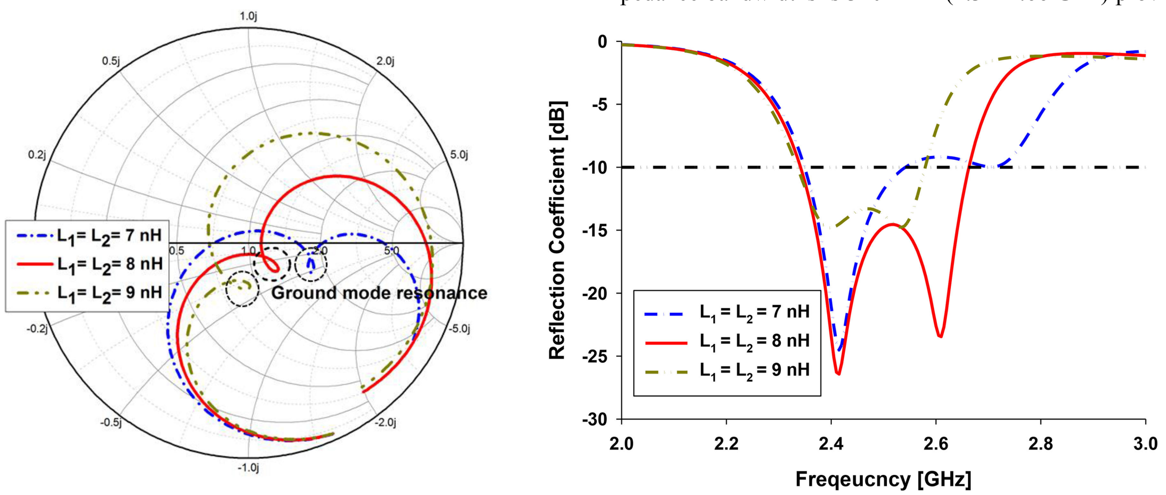

a b

Fig. 5 *Simulated results by varying the values of inductors ($L_1 = L_2$)*
(a) Simulated input impedance in a Smith chart, ***(b)*** Simulated reflection coefficients

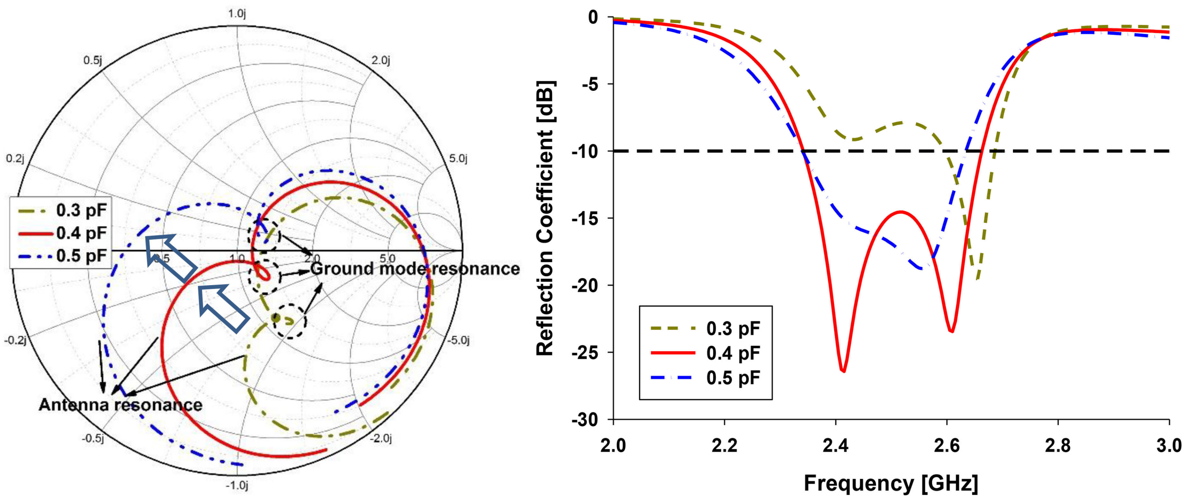

a b

Fig. 6 *Simulated results by varying the values of C_F*
(a) Simulated input impedance in a Smith chart, ***(b)*** Simulated reflection coefficients

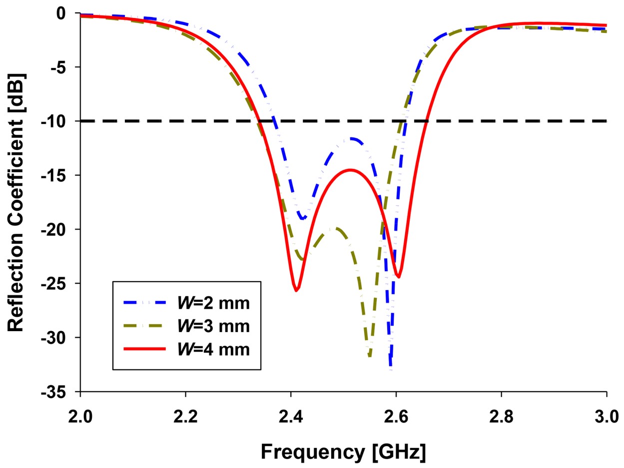

Fig. 7 *Simulated reflection coefficients with various widths (W) of the closed loop*

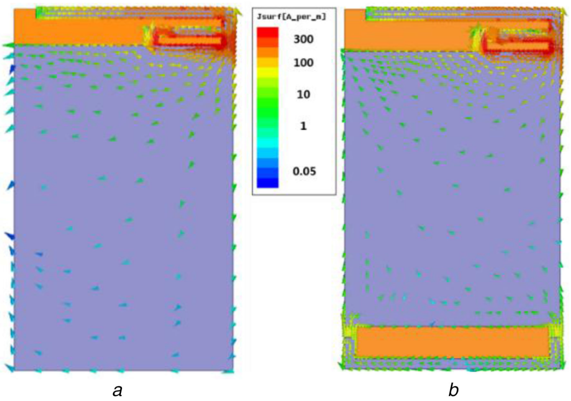

Fig. 8 *Simulated surface current distributions of antennas at 2.45 GHz*
(a) Reference antenna, ***(b)*** Proposed antenna

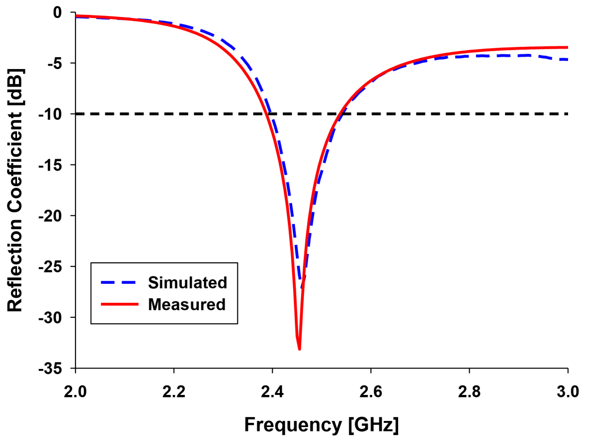

Fig. 9 *Simulated and measured reflection coefficients of the reference antenna*

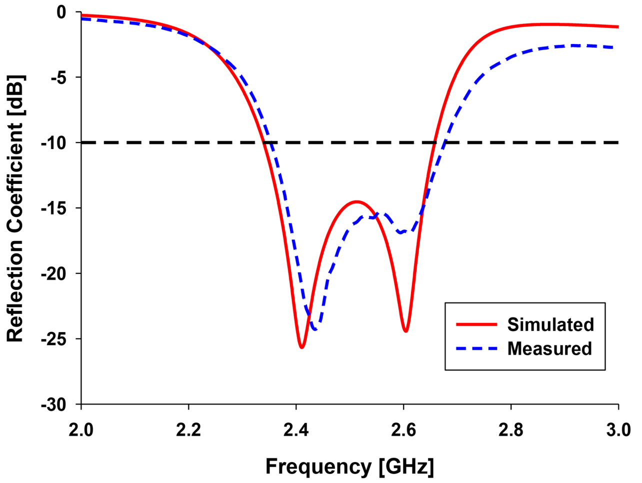

Fig. 10 *Simulated and measured reflection coefficients of the proposed antenna ($L_1 = L_2 = 8$ nH, $C_F = 0.4$ pF)*

best bandwidth performance. It can be concluded that larger size of the closed loop can achieve better performance.

The surface current distributions of the reference and proposed antennas at 2.45 GHz are compared in simulations as shown in Fig. 8. Large currents flow into the closed loop through the inductors, so the effective electrical length of the ground plane is enlarged, and this phenomenon gives a clear explanation of how the proposed technique works.

4 Experimental results

Fig. 9 shows the simulated and measured reflection coefficients of the reference antenna. The simulated −10 dB impedance bandwidth of the reference antenna without the closed loop is 140 MHz (2.39–2.53 GHz). As shown in Fig. 10, the simulated −10 dB impedance bandwidth of the proposed antenna ($L_1 = L_2 = 8$ nH, $C_F = 0.4$ pF) with the closed loop is 320 MHz (2.34–2.66 GHz), demonstrating that the impedance bandwidth with the closed loop is much wider than that of the reference antenna. In addition, the measured results agree well with the simulated ones, and the slight difference can be explained by experimental tolerance from the feeding cable [24, 25].

Fig. 11 shows the measured radiation patterns of the reference and proposed antennas in the *xy*-, *yz*- and *xz*-planes at 2.45 GHz. The peak gain of the proposed antenna is 2.3 dBi, whereas the peak gain of reference antenna is only 1.6 dBi, indicating that the peak gain is improved by ground mode tuning using the proposed closed loop. It can be observed that the radiation patterns for both antennas are basically omni-directional in the *xy*-plane, and the peak gain is improved when the proposed closed loop is added. These radiation patterns demonstrate that a dipole-type radiating current mode is generated along the *z*-axis of the ground plane, which is consistent with the theoretical analysis in Section 2.

Hand effect is a critical factor that can alter the radiation performance of the antenna, such as radiation patterns and efficiency, so that it is necessary to see the hand effect of the tuned ground plane. Fig. 12 shows the total efficiencies of the reference and proposed antennas in free space and with hand phantom measured from 2.3 to 2.6 GHz. The proposed antenna is placed in a cellular telecommunications & internet association (CTIA)-defined anthropomorphic hand phantom for bar style mobile phones for efficiency measurement [26, 27]. The measured efficiency of the proposed antenna ranges from 54 to 72% with average efficiency of 61%, whereas the average efficiency of the reference antenna ranges from 23 to 50%, averaging 36%. In measurement of hand phantom, the average efficiency of the reference antenna dropped from 36 to 17%, a degradation of 3.3 dB, while the proposed antenna dropped from 61 to 27%, a degradation of 3.6 dB. Since the acceptable degradation of antenna efficiency is approximately 3–5 dB in the high-frequency range against the free space [28, 29], the tunned ground plane is similarly sensitive to the hand phantom as the original ground plane. The proposed antenna seems to have 0.3 dB more or less in hand than the reference, and this may be explained by the location of the closed loop. More hand effect can be induced when the antenna structure and the closed loop are both close to the hand phantom. It is clear that the proposed antenna achieved higher efficiency than the reference antenna, indicating that improved radiation performance was obtained by using the proposed technique.

5 Conclusion

In this paper, we propose a PIFA with a controlled ground plane mode for performance improvement in the 2.4 GHz WLAN band. The 4 mm × 20 mm closed loop with lumped inductors is

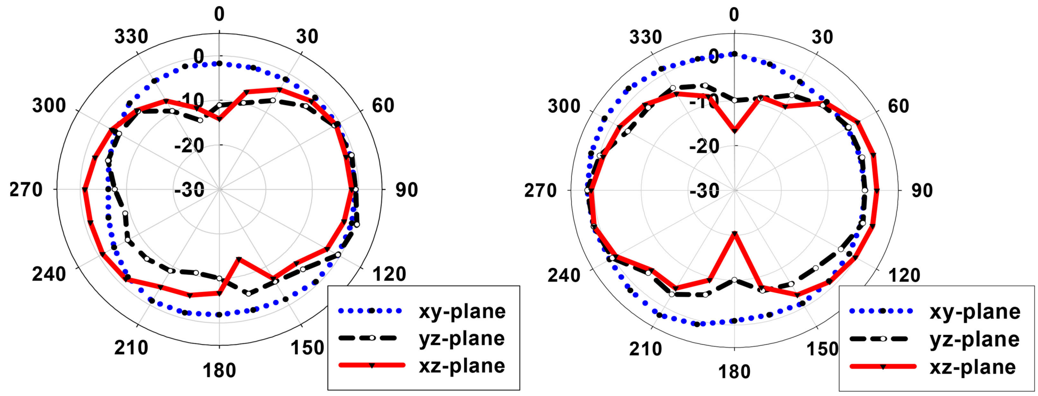

a *b*

Fig. 11 *Measured radiation patterns at 2.45 GHz*
(a) Radiation patterns of the reference antenna, ***(b)*** Radiation patterns of the proposed antenna

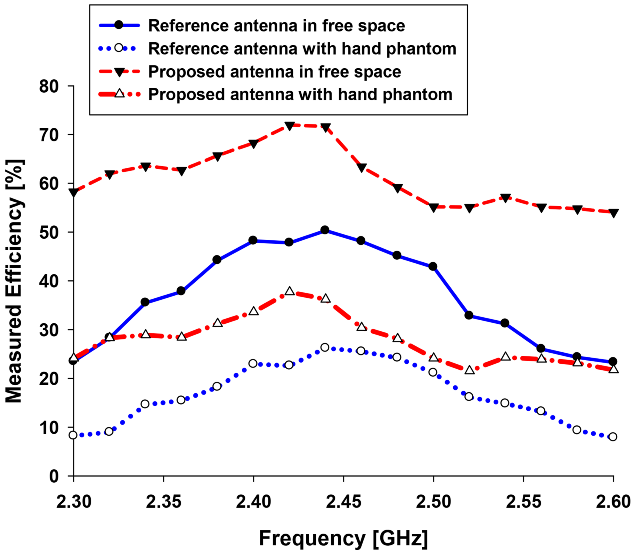

Fig. 12 *Measured efficiencies of reference and proposed antennas in free space and with hand phantom*

connected to the end of a small ground plane for ground mode control so that stronger coupling is generated between the antenna and the ground plane. Lumped inductors are adopted to achieve compact size and easy control of the ground mode resonance without changing the loop size. Strong coupling is generated between the antenna and the ground plane, and the ground resonance mode can be observed in a Smith chart, providing a wide impedance bandwidth and good radiation efficiency. The −10 dB bandwidth is considerably improved from 140 MHz (from 2.39 to 2.53 GHz) without the closed loop to 320 MHz (from 2.34 to 2.66 GHz) with the closed loop. The radiation patterns are basically omni-directional, which is suitable for mobile antennas. Furthermore, the measured total efficiency is also considerably improved, indicating enhanced antenna performance. The proposed technique is versatile and can be applied to different frequencies for different antennas.

6 Acknowledgments

This work was supported by the National Research Foundation of Korea (NRF) grant funded by the Korea government (MSIP) (grant no. 2015R1A2A1A15055109).

7 References

[1] Rowell, C., Lam, E.Y.: ‘Mobile-phone antenna design’, *IEEE Antenna Propag. Mag.*, 2012, **54**, (4), pp. 14–34

[2] Qu, L., Zhang, R., Kim, H.H., *et al.*: ‘Compact dual-band antenna using inverted-L loop and inner rectangular loop for WLAN applications’, *IET Electron. Lett.*, 2015, **51**, (23), pp. 1843–1844

[3] Qu, L., Zhang, R., Lee, H., *et al.*: ‘Compact triple-band ground radiation antenna using two inner rectangular loops enclosed by two outer loops’, *IET Electron. Lett.*, 2016, **52**, (10), pp. 790–792

[4] Wheeler, H.A.: ‘Fundamental limitations of small antennas’, *Proc. IRE*, 1947, **35**, (12), pp. 1479–1484

[5] Wheeler, H.A.: ‘Small antennas’, *IEEE Trans. Antennas Propag.*, 1975, **23**, (4), pp. 462–469

[6] Collin, R.E.: ‘Minimum Q of small antennas’, *J. Electromagn. Waves Appl.*, 1998, **12**, (10), pp. 1369–1393

[7] Harrington, R.F.: ‘Effect of antenna size on gain, bandwidth and efficiency’, *J. Res. Natl Bureau Standards D Radio Propag.*, 1960, **64D**, pp. l–12

[8] Lindberg, P., Ojefors, E., Rydberg, A.: ‘Wideband slot antenna for low-profile hand-held terminal applications’. European Conf. on Wireless Technology, Manchester, UK, September 2006, pp. 403–406

[9] Yousaf, J., Jung, H., Kim, K., *et al.*: ‘Design, analysis, and equivalent circuit modeling of dual band PIFA using a stub for performance enhancement’, *J. Electromag. Eng. Sci.*, 2016, **16**, (3), pp. 169–181

[10] Schroeder, W.L., Famdie, C.T., Solbach, K.: ‘Utilisation and tuning of the chassis modes of a handheld terminal for the design of multiband radiation characteristics’. IEE Conf. on Wideband and Multiband Antennas and Arrays, Birmingham, UK, September 2005, pp. 117–121

[11] Vainikainen, P., Ollikainen, J., Kivekas, O., *et al.*: ‘Resonator-based analysis of the combination of mobile handset antenna and chassis’, *IEEE Trans. Antennas Propag.*, 2002, **50**, (10), pp. 1433–1444

[12] Harrington, R.F.: ‘*Time-harmonic electromagnetic fields*’ (Wiley IEEE Press, 2001, 2nd edn.)

[13] Qu, L., Zhang, R., Shin, H., *et al.*: ‘Performance enhancement of ground radiation antenna for Z-wave applications using tunable metal loads’, *IET Electron. Lett.*, 2016, **52**, (22), pp. 1827–1828

[14] Qu, L., Zhang, R., Shin, H., *et al.*: ‘Mode-controlled wideband slot-fed ground radiation antenna utilizing metal loads for mobile applications’, *IEEE Trans. Antennas Propag.*, 2017, **65**, (2), pp. 867–872

[15] Harrington, R.F., Mautz, J.R.: ‘Theory of characteristic modes for conducting bodies’, *IEEE Trans. Antennas Propag.*, 1971, **19**, (5), pp. 622–628

[16] Huang, L., Schroeder, W.L., Russer, P.: ‘Estimation of maximum attainable antenna bandwidth in electrically small mobile terminals’. European Microwave Conf., Manchester, UK, September 2006, pp. 630–663

[17] Jeon, J., Zahid, Z., Kim, H.: ‘Dual band loop-type ground radiation antenna for mobile devices’, *Microw. Opt. Technol. Lett.*, 2016, **58**, (3), pp. 666–668

[18] Liu, Y., Kim, H.H., Kim, H.: ‘Loop-type ground radiation antenna for dual-band WLAN applications’, *IEEE Trans. Antennas Propag.*, 2013, **61**, (9), pp. 4819–4823

[19] Moon, S., Lee, H., Kim, H.: ‘A wideband loop-type antenna’, *Microw. Opt. Technol. Lett.*, 2015, **57**, (7), pp. 1742–1744

[20] Pozar, D.M.: ‘*Microwave engineering*’ (John Wiley & Sons, Inc., 2011, 4th edn.), pp. 272–277

[21] Kajfez, D.: ‘Dual resonance’, *IEE Proc., Microwave Antennas and Propagation*, 1988, **135**, (2), pp. 141–143

[22] Vilanen, J., Vainikainen, P.: ‘Optimum dual-resonant impedance matching of coupling element based mobile terminal antenna structures’, *Microw. Opt. Technol. Lett.*, 2007, **49**, (10), pp. 2472–2477

[23] Witt, F.J.: ‘Optimum lossy matching networks for resonant antennas’. IEEE Antennas and Propagation Society Int. Symp., San Jose, USA, Jun 1989, vol. **3**, pp. 1360–1363

[24] Chen, Z.N., Yang, N., Guo, Y.X., *et al.*: ‘An investigation into measurement of handset antennas’, *IEEE Trans. Instrum. Meas.*, 2005, **54**, (3), pp. 1100–1110

[25] Cao, Y.F., Cheung, S.W., Yuk, T.I.: ‘A multiband slot antenna for GPS/WiMAX/WLAN systems’, *IEEE Trans. Antennas Propag.*, 2015, **63**, (3), pp. 952–958

[26] Li, C.H., Douglas, M., Ofli, E., *et al.*: ‘Influence of the hand on the specific absorption rate in the head’, *IEEE Trans. Antennas Propag.*, 2012, **60**, (2), pp. 1066–1074

[27] ‘CTIA: The Wireless Association’, http://files.ctia.org/pdf/CTIA_OTA_Test_plan_Rev_3.1.pdf, accessed 05 January 2017

[28] Lee, J., Lee, J., Min, K., *et al.*: 'Miniaturized antennas with reduced hand effects in mobile phones using magneto-dielectric material', *IEEE Antennas Wirel. Propag. Lett.*, 2014, **13**, pp. 935–938

[29] Hsu, C.K., Chung, S.J.: 'Compact multiband antenna for handsets with a conducting edge', *IEEE Trans. Antennas Propag.*, 2015, **63**, (11), pp. 5102–5107